JBC RESEARCH ARTICLE

Macrophages bind LDL using heparan sulfate and the perlecan protein core

Received for publication, December 10, 2020, and in revised form, March 3, 2021 Published, Papers in Press, March 5, 2021,
https://doi.org/10.1016/j.jbc.2021.100520

Chun-yi Ng[1,2,3], John M. Whitelock[1], Helen Williams[2,3], Ha Na Kim[1], Heather J. Medbury[2,3,*], and Megan S. Lord[1,*]

From the [1]Graduate School of Biomedical Engineering, UNSW Sydney, Sydney, New South Wales, Australia; [2]Vascular Biology Research Centre, Department of Surgery, Westmead Hospital, Westmead, New South Wales, Australia; and [3]The University of Sydney, Westmead Clinical School, Westmead, New South Wales, Australia

Edited by Gerald Hart

The retention of low-density lipoprotein (LDL) is a key process in the pathogenesis of atherosclerosis and largely mediated *via* smooth-muscle cell-derived extracellular proteoglycans including the glycosaminoglycan chains. Macrophages can also internalize lipids *via* complexes with proteoglycans. However, the role of polarized macrophage-derived proteoglycans in binding LDL is unknown and important to advance our understanding of the pathogenesis of atherosclerosis. We therefore examined the identity of proteoglycans, including the pendent glycosaminoglycans, produced by polarized macrophages to gain insight into the molecular basis for LDL binding. Using the quartz crystal microbalance with dissipation monitoring technique, we established that classically activated macrophage (M1)- and alternatively activated macrophage (M2)-derived proteoglycans bind LDL *via* both the protein core and heparan sulfate (HS) *in vitro*. Among the proteoglycans secreted by macrophages, we found perlecan was the major protein core that bound LDL. In addition, we identified perlecan in the necrotic core as well as the fibrous cap of advanced human atherosclerotic lesions in the same regions as HS and colocalized with M2 macrophages, suggesting a functional role in lipid retention *in vivo*. These findings suggest that macrophages may contribute to LDL retention in the plaque by the production of proteoglycans; however, their contribution likely depends on both their phenotype within the plaque and the presence of enzymes, such as heparanase, that alter the secreted protein structure.

Atherosclerosis is a chronic, complex inflammatory disease that occurs in the vascular wall. It is initiated by the subendothelial retention of low-density lipoprotein (LDL) from the bloodstream. This is largely mediated *via* extracellular proteoglycans including the glycosaminoglycan chains (1–3), initially those secreted by resident smooth muscle cells (4, 5). LDL may be modified by oxidation, glycation, aggregation, or incorporation into immune complexes with susceptibility to modification increased when bound to proteoglycans as a result of irreversible structural changes (6, 7). Thus, the binding of LDL to proteoglycans is a key event in atherogenesis. Recruitment of monocytes, differentiation into macrophages, and subsequent uptake of oxidized LDL (oxLDL)-proteoglycan complexes are major events underlying the progression of atherosclerosis and accelerating plaque formation (8–10). In particular, oxidation of LDL leads to recognition by scavenger receptors on the surface of macrophages that promote the internalization of oxLDL-proteoglycan complexes, a process that leads to the formation of foam cells. In addition, modified LDL is chemotactic for monocytes, further supporting disease progression, including by this pathway as macrophages also produce proteoglycans that may contribute to the continued retention of LDL that occurs throughout atherosclerosis development (7, 11).

Proteoglycans are proteins that are posttranslationally modified with linear polysaccharide chains called glycosaminoglycans. Glycosaminoglycans are composed of repeating disaccharide units modified with sulfate groups at various positions. Glycosaminoglycan family members include chondroitin sulfate (CS), dermatan sulfate, keratan sulfate, heparan sulfate (HS), and heparin. In addition, hyaluronan is a glycosaminoglycan; however, it is synthesized at the cell membrane and does not decorate a core protein (12). Sulfated glycosaminoglycans bind LDL *via* electrostatic interactions, with the dense negative sulfated regions of glycosaminoglycans binding clusters of basic amino acids in the protein component of LDL, apolipoprotein B-100 (13–16). LDL has the highest affinity for heparin, the glycosaminoglycan with the highest level of sulfation (17, 18), while dermatan sulfate, HS, and CS, with a lower level of sulfation, exhibit a lower affinity. HS is reported to bind LDL to a similar extent as CS; however, the sulfate content in the HS preparation used contained less than half the level of sulfation as CS (15). Interestingly, LDL has a higher affinity for glycosaminoglycan chains when presented in their proteoglycan form compared with isolated chains, consistent with their native presentation in the vascular wall (19). The binding of LDL to proteoglycans and formation of oxLDL-proteoglycan complexes enhance lipid internalization *via* scavenger receptors on macrophages (20–22) and hence are involved in the progression of atherosclerotic plaques.

* For correspondence: Heather J. Medbury, heather.medbury@sydney.edu.au; Megan S. Lord, m.lord@unsw.edu.au.

Macrophages bind LDL using HS and perlecan

To date, much of the understanding of the structure of proteoglycans in the arterial wall and the interaction with LDL has been derived from arterial smooth muscle cells and endothelial cells (4, 5, 9, 23). CS proteoglycans including biglycan, decorin, and versican are abundant in the vascular wall during atherosclerosis and bind LDL (16, 24–27). Deletion of one of the CS enzymes involved in chain elongation, CS N-acetylgalactosaminyltransferase-2, reduced LDL retention in a mouse model of diffuse intimal thickening (28) confirming the physiological role of CS in lipid binding. Perlecan, an HS proteoglycan, is abundant in the normal vascular basement membrane; however, its expression in this region is decreased during atherosclerosis (29, 30). Perlecan, however, is highly expressed in both the necrotic core and fibrous cap of advanced plaques (31) and can bind LDL, suggesting a lipid-binding role for perlecan in the plaque (32).

The altered microenvironment within the vascular wall during atherosclerosis, such as increased infiltration of monocytes, which differentiate into macrophages, as well as activation of smooth muscle cells, suggests that these cells may contribute to proteoglycan-mediated lipid retention (25). For example, transforming growth factor-β1 signals smooth muscle cells to synthesize proteoglycans with longer glycosaminoglycan chains that exhibit an increased affinity for LDL compared with proteoglycans synthesized by quiescent cells (5, 33, 34).

Macrophages also secrete proteoglycans that bind LDL (19, 24, 25, 35). Macrophages cultured *in vitro* under hypoxic conditions to simulate the plaque environment increase versican and perlecan expression, and their affinity for LDL, owing to their longer glycosaminoglycan chains with increased sulfation (36, 37). Although the phenotype of these macrophages was not described, these studies suggest that macrophages in the atherosclerotic plaque can alter their synthesis of proteoglycans, which in turn could influence LDL binding and oxidation.

Macrophages exhibit pro- or anti-inflammatory properties depending on the cytokines present in their microenvironment (38). Polarization of macrophages can be achieved *via* classical activation with interferon-γ (IFN-γ) and lipopolysaccharide (LPS) to produce proinflammatory or M1 macrophages while alternative activation with interleukin (IL)-4 produces anti-inflammatory, reparative, or M2 macrophages (39–41). Both M1 and M2 macrophages are present within plaques with both types found within the fibrous cap while M1 dominates in the shoulder regions and M2 dominates in the adventitia (42–44). While M1 macrophages are associated with plaque instability, M2 macrophages provide structural integrity to the plaque (44). This raises the prospect of stabilizing plaques by modulating the balance of resident M1/M2 macrophages (45). Indeed, this has been shown in mice (46). However, the utility of this approach requires an understanding of the contribution of macrophage subsets to proteoglycan secretion and LDL binding. Therefore, this study aimed to examine the proteoglycans, and pendent glycosaminoglycans, produced by M1 and M2 polarized macrophages and to examine their role in LDL binding.

Results

Glycosaminoglycans are present in human atherosclerotic plaques

As the glycosaminoglycan chains of proteoglycans have been established to bind LDL and assist in its internalization by macrophages, it was of interest to determine the pattern of expression of the major glycosaminoglycans, namely CS and HS, in advanced human carotid atherosclerotic plaques. The

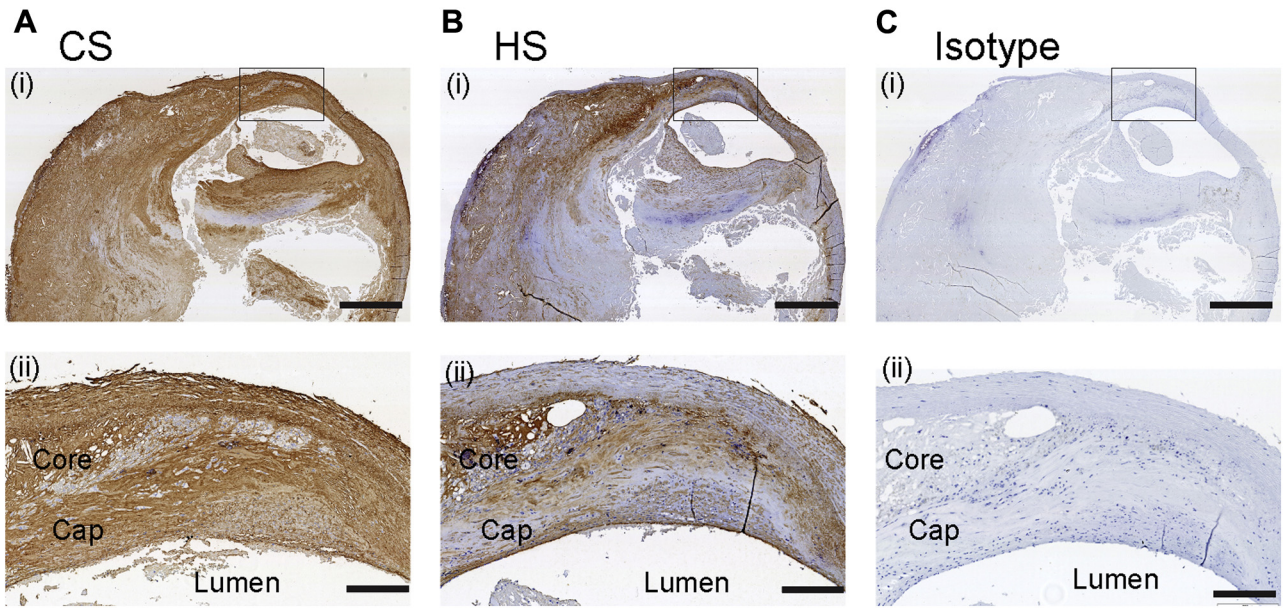

Figure 1. CS and HS are localized in the core and cap of late atherosclerotic plaques. Representative micrographs showing the localization of (*A*) CS and (*B*) HS compared with the (*C*) isotype control at (*i*) low and (*ii*) higher magnification of the boxed area indicated in (*i*). HS was probed with the monoclonal anti-HS chain antibody (clone 10E4) and CS was probed with the monoclonal anti-CS antibody (clone CS-56). Antibody binding was visualized with DAB (*brown*) and nuclei were counterstained with hematoxylin (*blue*). *Scale bar* is 1 mm in (*i*) and 200 μm in (*ii*).

plaques displayed a well-formed fibrous cap over the necrotic core comprising macrophage foam cells (Fig. 1). CS was distributed throughout the plaque (Fig. 1*A* (i)), both in the fibrous cap and in the necrotic core (Fig. 1*A* (ii)). In addition, HS was abundant in the necrotic core with weaker staining exhibited in the fibrous cap (Fig. 1*B* (i) and (ii)). The isotype control did not show any positive staining, indicating that the CS and HS staining was specific (Fig. 1*C*). These results indicated that both CS and HS were present in the lipid-rich necrotic core.

Human monocytic cell line, THP-1, as a model for primary human cells

The use of primary macrophages for proteoglycan biochemical and lipid binding characterization is prohibitive due to the number of cells that can be isolated and their limited survival in culture. The human monocytic THP-1 cell line was investigated as a model for primary cells as it exhibits the morphological and functional properties of primary cells (47, 48). THP-1 cells were examined for their ability to be polarized into M1 and M2 phenotypes in a similar way to primary macrophages. Although the THP-1 cells polarized by LPS and IFN-γ to the M1 phenotype, and by IL-4 to the M2 phenotype, did not exhibit as strong a degree of skewing as the primary cells, they still exhibited a shift to higher CD86 and lower CD11b expression in the M1 compared with M2 macrophages consistent with the primary cells (Fig. S1, *A* and *B*). Furthermore, light microscopy images revealed the similarity of the morphological appearance of both the primary and THP-1 cells polarized into M1 macrophages with a spindle-shaped appearance or M2 macrophages with a rounded morphology (Fig. S1*C*). Thus, the THP-1 cells were able to be polarized to either the M1 or M2 phenotype comparable to primary macrophages.

M1 and M2-polarized primary and THP-1 cells differentially express proteoglycans and glycosaminoglycans

The proteoglycans secreted by primary and THP-1-derived macrophages displaying either the M1 or M2 phenotype were also examined. Both primary and THP-1 cells were cultured under conditions to induce either the M1 or M2 phenotype and the proteoglycans produced were isolated from the conditioned medium pooled from these cultures over several medium exchanges by anion exchange chromatography (Fig. S2). A comparison of chromatography elution profiles indicated that there was less protein eluted from the primary and foam cell preparations compared with the THP-1 preparations (Fig. S2*A*); however, when this was adjusted for the protein yield, there was no difference between primary and THP-1 preparations for the M1 and M2-polarized cells (Fig. S2*B*). The protein yield from the M1 and M2 THP-1 foam cell preparations was low.

Mass spectrometry analyses of the proteoglycans in each of these samples revealed that the macrophages produced a range of extracellular and cell surface proteoglycans (Table 1). Interestingly, primary M1 macrophages secreted aggrecan, biglycan, inter-α-trypsin inhibitor, lumican, mimecan, perlecan, versican, and chondroitin sulfate proteoglycan 4 (CSPG4). M1 THP-1 macrophages also secreted these proteoglycans, except for versican and CSPG4. In addition, M1 THP-1 macrophages secreted agrin, syndecan-4, and serglycin, which were not expressed by the primary cells. M2 primary macrophages secreted aggrecan, inter-α-trypsin inhibitor, lumican, mimecan, perlecan, CSPG4, and serglycin. M2 THP-1 macrophages also secreted these proteoglycans, apart from biglycan, mimecan, CSPG4. In addition, M2 THP-1 macrophages secreted agrin, versican, glypican-4, and syndecan-2. Thus, there were some differences in the proteoglycan

Table 1
M1 and M2-polarized primary and THP-1 cells differentially express proteoglycans

			MOWSE score (peptides identified, % sequence coverage)			
			M1		M2	
	Protein	Accession number	Primary	THP-1	Primary	THP-1
Extracellular	Aggrecan	NP_001126	130 (3, 1.4)	234 (7, 3.8)	200 (3, 1.4)	124 (2, 1.2)
	Agrin	NP_940978		715 (17, 15)		1024 (17, 15)
	Biglycan	NP_001702	112 (3, 16)	128 (3, 16)	88 (2, 6.0)	
	Inter-α-trypsin inhibitor					
	Heavy chain 1	NP_002206	289 (3, 4.1)	102 (1, 1.7)	329 (5, 4.6)	128 (2, 1.7)
	Heavy chain 2	NP_002207	977 (11, 6.7)	263 (5, 6.6)	865 (13, 12)	262 (6, 7.6)
	Heavy chain 3	NP_002208	439 (8, 7.9)	163 (5, 5.4)	481 (6, 6.0)	180 (3, 3.4)
	Lumican	NP_002336	534 (6, 17)	533 (4, 14)	450 (5, 14)	430 (8, 21)
	Mimecan	NP_054776	295 (4, 14)	74 (1, 7.1)	202 (4, 17)	
	Perlecan	NP_005520	657 (8, 3.4)	435 (6, 2.0)	853 (12, 3.5)	346 (7, 2.8)
	Versican	NP_004376	108 (3, 1.1)			94 (1, 0.6)
Cell surface	Chondroitin sulfate proteoglycan 4 (CSPG4)	NP_001888	219 (5, 2.7)	72 (2, 0.8)	244 (6, 3.4)	
	Glypican-4	NP_001439				164 (2, 9.2)
	Syndecan-2	NP_002989				261 (2, 8.5)
	Syndecan-4	NP_002990		74 (1, 8.1)		
Intracellular	Serglycin	NP_002718		172 (4, 34)	102 (2, 23)	192 (4, 26)

Proteoglycan-enriched conditioned medium from polarized primary and THP-1 cells was analyzed by peptide LC-MS2 from an in-solution tryptic digest and presented in alphabetical order and grouped into extracellular, cell surface, and intracellular proteins. Confidence of peptide identity was assessed by the MOWSE score greater than 70. The number of unique peptide matches and % sequence coverage are indicated in parentheses.

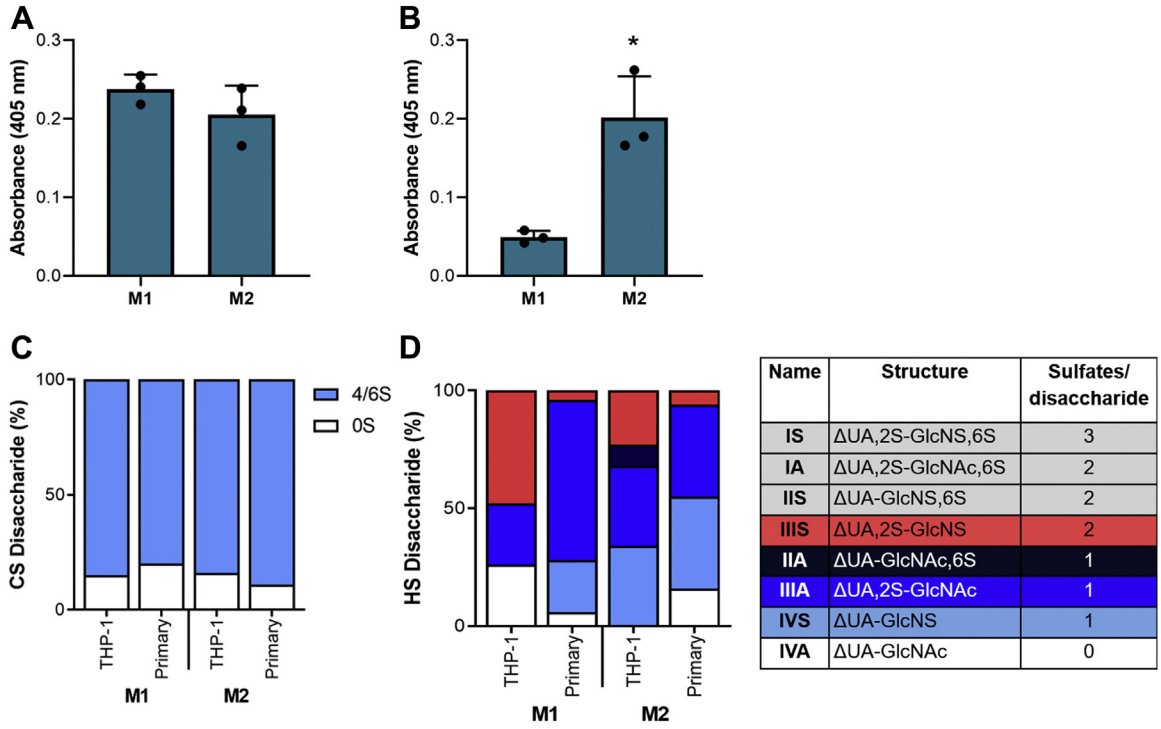

Name	Structure	Sulfates/ disaccharide
IS	ΔUA,2S-GlcNS,6S	3
IA	ΔUA,2S-GlcNAc,6S	2
IIS	ΔUA-GlcNS,6S	2
IIIS	ΔUA,2S-GlcNS	2
IIA	ΔUA-GlcNAc,6S	1
IIIA	ΔUA,2S-GlcNAc	1
IVS	ΔUA-GlcNS	1
IVA	ΔUA-GlcNAc	0

Figure 2. M1 and M2-polarized primary and THP-1 cells differentially express glycosaminoglycans. *A*, the presence of CS chains produced by the THP-1 cells using mouse monoclonal antibody clone CS-56 determined by ELISA (n = 3). *B*, the presence of HS chains produced by the THP-1 cells using mouse monoclonal antibody clone 10E4 determined by ELISA (n = 3). *Asterisk* indicates significant difference compared with M1. *C*, proportion of CS disaccharides present in proteoglycan-enriched medium conditioned elaborated by M1 and M2-polarized primary and THP-1 cells. *D*, proportion of HS disaccharides present in proteoglycan-enriched medium conditioned elaborated by M1 and M2-polarized primary and THP-1 cells. The HS disaccharide structures are indicated by both their abbreviated name and structure (table inset).

protein core expression profiles between primary and THP-1 macrophage phenotypes.

The conditioned medium from each of the cultures was further analyzed for the presence and structure of the glycosaminoglycans (Fig. 2). Analysis of the relative abundance of CS and HS secreted by THP-1 macrophages was determined by ELISA using antibodies raised against epitopes commonly found on either CS or HS. This analysis revealed a similar level of CS epitopes produced by both M1 and M2 macrophages while M2 macrophages produced significantly more HS epitopes than M1 macrophages (Fig. 2, *A* and *B*). Furthermore, the CS produced by both primary and THP-1 macrophages, whether displaying an M1 or M2 phenotype, was primarily composed of monosulfated disaccharides, either 4- or 6-sulfated, while only 10–20% of the chains were unsulfated (Figs. 2*C* and S3*A*). In contrast, the HS profile was different between the primary and THP-1 macrophage phenotypes. M1 THP-1 macrophage-derived HS contained 50% disulfated disaccharides (ΔUA,2S-GlcNS), 25% monosulfated disaccharides (ΔUA,2S-GlcNAc), and 25% unsulfated disaccharides (ΔUA-GlcNAc) while M1 primary macrophage-derived HS contained 5% disulfated disaccharides (ΔUA,2S-GlcNS), 90% monosulfated disaccharides (ΔUA,2S-GlcNAc and ΔUA-GlcNS), and 5% unsulfated disaccharides (ΔUA-GlcNAc) (Figs. 2*D* and S3*B*). Additionally, M2 THP-1-derived HS contained 23% disulfated disaccharides (ΔUA,2S-GlcNS) and 77% monosulfated disaccharides (ΔUA-GlcNAc,6S, ΔUA,2S-GlcNAc, and ΔUA-GlcNS) while M2 primary macrophage-derived HS contained 5% disulfated disaccharides (ΔUA,2S-GlcNS), 80% monosulfated disaccharides (ΔUA,2S-GlcNAc and ΔUA-GlcNS), and 15% unsulfated disaccharides (ΔUA-GlcNAc) (Figs. 2*D* and S3*B*). These data indicated an overall higher level of sulfation for the HS produced by both M1 and M2 THP-1 macrophages than M1 and M2

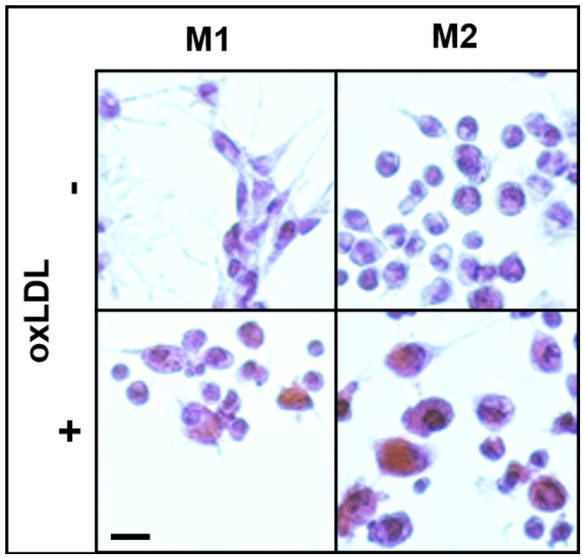

Figure 3. THP-1 cells with M1 and M2 phenotypes internalize oxLDL to become foam cells. Representative light microscopy images of oil red O stained M1 or M2-polarized THP-1 cells either untreated or treated with oxLDL to form foam cells. Scale bar represents 20 μm.

Table 2
THP-1-derived M1 and M2 foam cells differentially express proteoglycans

Protein		Accession number	MOWSE score (peptides identified, % sequence coverage)	
			M1	M2
Extracellular	Agrin	O00468		246 (7, 5.2)
	Lumican	NP_002336		123 (1, 5.6)
	Perlecan	NP_005520		548 (10, 4.2)
	Versican	NP_004376		111 (2, 1.0)
Cell surface	Syndecan-2	NP_002989	100 (1, 8.5)	299 (2, 8.5)
Intracellular	Serglycin	NP_002718	223 (4, 34)	636 (7, 38)

Proteoglycan-enriched conditioned medium from THP-1 cells polarized into M1 or M2 foam cells was analyzed by peptide LC-MS2 from an in-solution tryptic digest and presented in alphabetical order and grouped into extracellular, cell surface, and intracellular proteins. Confidence of peptide identity was assessed by the MOWSE score greater than 70. The number of unique peptide matches and % sequence coverage are indicated in parentheses.

primary macrophages. In addition, M1-derived HS was more sulfated than M2-derived HS.

THP-1 cell-derived foam cells differentially express proteoglycans and glycosaminoglycans

THP-1 cells were further investigated for their ability to internalize oxLDL and display the foam cell phenotype. M1 and M2 THP-1 macrophages were treated with oxLDL and found to internalize lipids as shown by the positive staining with Oil Red O as well as a more rounded morphology compared with untreated cells (Fig. 3). Mass spectrometry analyses of the proteoglycans in each of these samples revealed that M2 THP-1 foam cells secreted agrin, lumican, perlecan, versican, syndecan-2, and serglycin while M1 THP-1 foam cells only secreted syndecan-2 and serglycin (Table 2). These data support the conclusion of reduced secretion of proteoglycans by foam cells compared with the M1 and M2 macrophages (Tables 1 and 2).

Macrophage proteoglycans bind LDL via *HS and their protein core*

Having established that macrophage subsets secrete a range of proteoglycans decorated with both HS and CS, it was important to establish that these proteoglycans could bind LDL. This was performed in a turbidity assay as the binding of LDL to proteoglycans formed insoluble complexes in the presence of Ca^{2+} ions. Proteoglycans isolated from M1 and M2 THP-1 macrophages bound LDL over a range of proteoglycan concentrations (Fig. 4*A*). This binding was further explored by QCM-D to quantify the extent of binding where the proteoglycan fraction was adsorbed onto the gold sensor surface, blocked with albumin, and then exposed to LDL in the absence of divalent cations to minimize the formation of insoluble complexes. Each of these binding events was represented by a decrease in frequency, which is related to the amount of mass deposited, accompanied by increased dissipation, which is related to the viscoelasticity of the immobilized layer (Fig. 4*B*). The Δf and ΔD values for each experiment were input into the Voigt viscoelastic model to obtain adsorbed mass estimates for both the proteoglycans and LDL. These analyses indicated each proteoglycan fraction adsorbed to the gold sensor surface to approximately the same degree (554 ± 29 ng/cm^2) (Fig. 4*C*). LDL bound to all proteoglycan fractions from both primary and THP-1 cells (Fig. 4*D*). There was no significant difference in the level of LDL bound to proteoglycan fractions secreted by primary or THP-1 macrophages for either M1 or M2 subsets. However, proteoglycans secreted by M1 macrophages bound approximately 1.6-fold more LDL than the proteoglycans secreted by M2 macrophages (Fig. 4*D*).

LDL binding to these proteoglycan fractions was further investigated to establish the role of the glycosaminoglycan chains. Removal of HS and CS from the proteoglycan fraction by HepIII and C'ase ABC, respectively, was verified by ELISA (Fig. S4). Removal of CS from the proteoglycan fraction had no effect (Fig. 4*E*). In contrast, removal of HS resulted in a 2.9- and 7.1-fold reduction in LDL binding to primary and M1 THP-1 macrophage-derived proteoglycans, respectively, while additional removal of the CS had no additive effect (Fig. 4*E*). LDL binding to the M1 primary and THP-1-derived fractions treated to remove both HS and CS was approximately 14 and 34%, respectively of the LDL bound to intact fractions consistent with LDL binding to the core proteins (Fig. 4*E*). These data indicated that both HS and the protein cores were involved in LDL binding (Fig. 4*F*). Further, approximately half of the LDL bound to the M1 THP-1 macrophage-derived proteoglycans that had been treated to remove CS was *via* electrostatic interactions as treatment with 1 M NaCl resulted in a 1.8-fold reduction in LDL binding (Fig. 4*G*). Involvement of the HS and CS chains in LDL binding to the M2-derived proteoglycan fractions was similar to that for the M1-derived proteoglycan fractions (Fig. 4*H*). Removal of CS had no effect on the level of LDL binding while removal of HS supported a 4.8- and 3.7-fold reduction in LDL binding to M2 primary and THP-1-derived proteoglycans, respectively, while additional removal of the CS had no additive effect (Fig. 4*H*). LDL binding to the M2 primary and THP-1-derived fractions treated to remove both HS and CS was approximately 27% of the LDL bound to intact fractions consistent with LDL binding to the core proteins (Fig. 4*H*). These data indicated that both M2-derived HS and protein cores were involved in LDL binding (Fig. 4*F*). Comparison of the LDL adsorption behavior to the different M2 THP-1 proteoglycan preparations was performed by plotting ΔD *versus* Δf (D*f* plots; Fig. 4*I*). These plots indicated LDL binding to the control proteoglycan fraction as detected by decreased Δf and increased ΔD. In contrast, the D*f* plot for LDL binding to the proteoglycan preparation devoid of both HS and CS exhibited a decrease in

Δf with little change in ΔD throughout the measurement period consistent with a lower level of binding and more rigid binding, consistent with protein core binding. Thus, the different protein and glycosaminoglycan compositions of the proteoglycan fraction from each macrophage subset determined the relative extent of LDL binding between protein and glycosaminoglycan components.

LDL binds to the protein core of perlecan

As the binding of LDL to the proteoglycan fractions involved the core proteins, further assessment was conducted to identify which proteoglycans were involved. The QCM-D experimental setup to quantify LDL binding to M2 THP-1-derived proteoglycans (Fig. 4*B*) was extended to add an antibody to a selected proteoglycan core protein prior to the addition of LDL (Fig. 5*A*). Polyclonal antibodies raised against core proteins of perlecan or versican were selected as these proteoglycans were present in the proteoglycan fractions (Table 1) and previously associated with LDL binding (36, 37). In addition, a polyclonal antibody raised against biglycan (core protein) was used as a control as biglycan was not found in the M2 THP-1-derived proteoglycan fraction (Table 1). The M2 THP-1-derived proteoglycans were treated to remove both CS and HS prior to immobilization to assess the effect of each antibody on the level of LDL binding to the protein core. The anti-perlecan antibody reduced LDL binding to this fraction 4.6-fold while the anti-versican and anti-biglycan antibodies had no effect (Fig. 5*B*). These data suggested that perlecan present in the M2-derived fractions supported LDL binding. Western blotting indicated the presence of full-length perlecan in the M2 THP-1-dervied proteoglycan fraction with a 460 kDa core protein decorated with HS, as shown by the small shift in immunoreactivity in the absence of HS, but not CS (Fig. 5*C*). The M2 THP-1-derived proteoglycan fraction was further enriched for perlecan *via* immunoaffinity chromatography and its purity confirmed *via* both ELISA and mass spectrometry (Fig. S5 and Table S1). The flow through fraction was also examined to confirm that it did not contain perlecan. LDL bound to the M2 THP-1-derived perlecan, while the level of LDL binding was 4.2-fold greater in the absence of HS (Fig. 5*D*). In contrast, LDL did not bind to the proteins present in the M2 THP-1 fraction depleted of perlecan and glycosaminoglycans. Human primary aortic endothelial cell perlecan, which is exclusively decorated with HS (49), also bound LDL *via* its protein core and supported a 2.2-fold higher level of LDL binding in the absence of HS (Fig. 5*D*). Furthermore, addition of the polyclonal anti-perlecan antibody prior to exposure to LDL binding inhibited LDL binding to endothelial perlecan (Fig. 5*D*). These data suggested that perlecan was the major proteoglycan secreted by M2 THP-1 macrophages that bound LDL bound *via* the protein core (Fig. 5*E*).

Perlecan colocalizes with M2 macrophages in late atherosclerotic plaques

As perlecan was found to be major contributor to LDL binding in the M2 macrophage-derived proteoglycan fraction, the colocalization of perlecan and M2 macrophages within human late atherosclerotic plaques was investigated. Perlecan was localized to both the fibrous cap and the necrotic core where M2 macrophages were also present (Fig. 6). In addition, some of the M2 macrophages identified colocalized with perlecan (Fig. 6, *B* and *C*).

Discussion

This study demonstrated that macrophages, whether primary or from the THP-1 cell line, secreted a range of proteoglycans that bound LDL *via* their glycosaminoglycan and/or protein components. The THP-1 cell line has previously been established as a model of human monocyte-derived macrophages with the ability to be polarized to M1 and M2 phenotypes (48) and was thus used in this study as a more abundant source of polarized macrophage-derived proteoglycans and compared, where possible, with proteoglycans secreted by primary cells. The polarization of the THP-1 cell line to the M1 phenotype was not as marked as for primary cells. It is acknowledged that macrophage phenotype is a spectrum and there are differences in the degree of polarization toward M1 or M2 phenotypes when exposed to the same stimulus (50).

Interestingly, M1 and M2-polarized macrophages secreted proteoglycans that bound LDL as determined by a turbidity assay in the presence of Ca^{2+} ions that promoted the formation of insoluble complexes, extending previous studies (2). The QCM-D was used in this study for the first time as a more sensitive technique to study LDL interactions with proteoglycans in conditions that did not support the formation of insoluble complexes and revealed that macrophage-derived proteoglycans bound LDL *via* both their protein core and HS. These findings extend previous reports that macrophages secrete proteoglycans that bind LDL (19, 24, 25, 35) and provide context for the relative contribution of proteoglycans produced by polarized macrophages.

Macrophages have previously been shown to secrete proteoglycans including agrin, decorin, glypican-4, perlecan, syndecans-1–4, and versican (37, 51–53), with this study extending this list to include aggrecan, inter-a-trypsin inhibitor, lumican, mimecan, and CSPG4. As several of these proteoglycans can bind LDL, it suggests that macrophages may contribute to LDL binding in the plaque by secretion of an array of proteoglycans. Notably, foam cells derived from either M1 or M2-polarized macrophages reduced their secretion of proteoglycans, which may be attributed to the cytotoxic effect of oxLDL internalization (54, 55). This implies that once a foam cell forms, as is the case in advanced plaques, they reduce secretion of proteoglycans that could play a role in the retention of newly deposited LDL from the circulation.

CS was abundantly expressed in the advanced human atherosclerotic plaques analyzed in this study and binds LDL (16, 24–27). Multiple CS proteoglycans have been localized to the macrophage-rich plaque core including decorin, biglycan, and versican (56, 57). The present study found that macrophages secrete CS proteoglycans including biglycan and versican, but not decorin. The CS secreted by either macrophage phenotype did not bind LDL and mostly contained

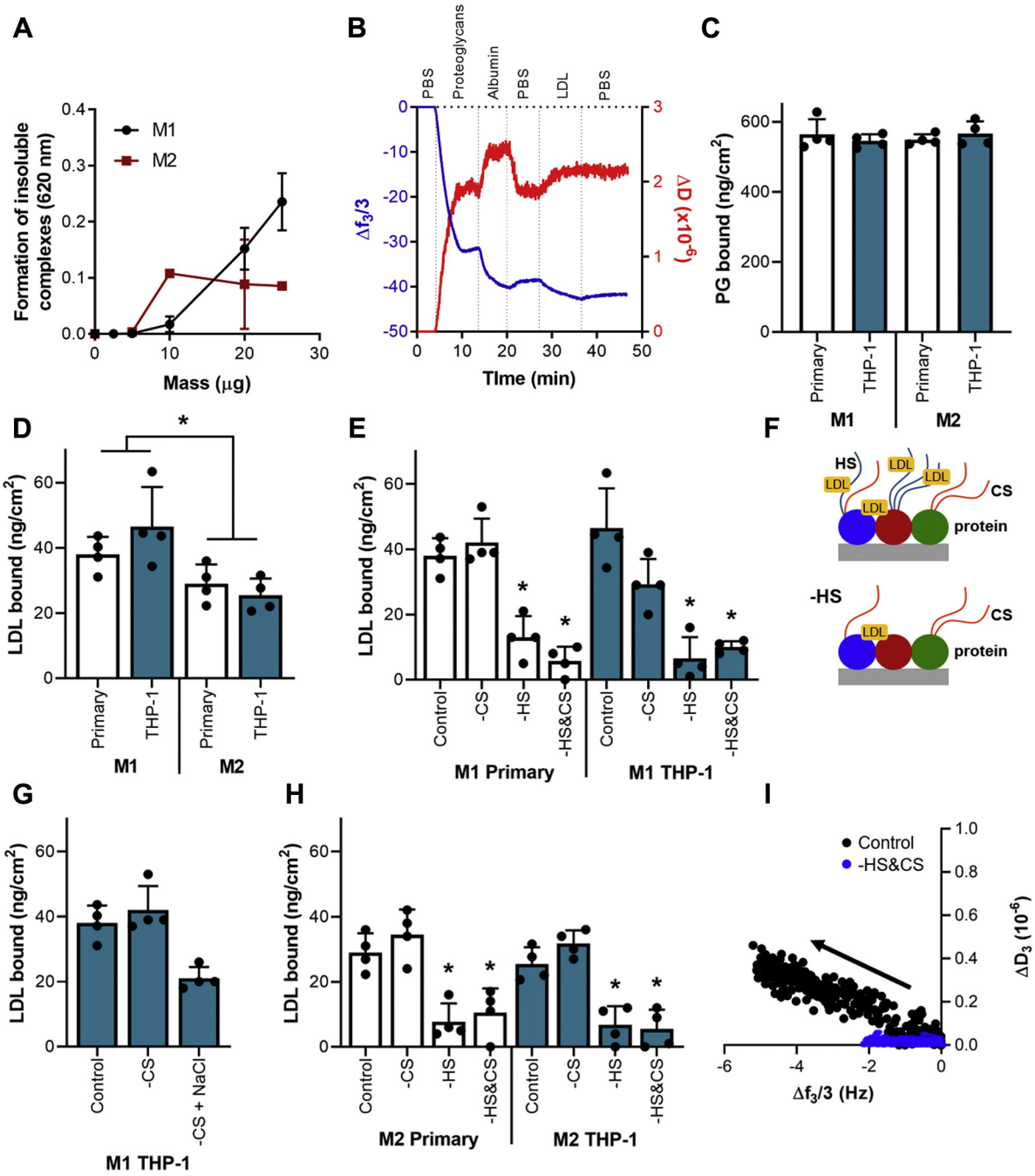

Figure 4. Macrophage proteoglycans bind LDL *via* HS and their protein core. *A*, determination of LDL binding to M1 and M2 THP-1 proteoglycans by turbidity measurement over a range of proteoglycan doses. Data are presented as mean ± SD (n = 3). *B*, sample QCM-D experiment of LDL binding to M1 THP-1 proteoglycans displayed as changes in frequency (Δ*f*) and dissipation (ΔD) *versus* time for the third overtone. The vertical lines indicate the addition of PBS, proteoglycans, albumin, or LDL. *C*, mass of proteoglycan fractions bound to sensor surface. The mass of proteoglycan (PG) bound was determined by Voigt modeling of the QCM-D data. Data are presented as mean ± SD (n = 4). Mass of LDL bound to proteoglycans elaborated by (*D*) different primary and THP-1 macrophage subsets or (*E*) M1-polarized primary and THP-1 cells. The mass of LDL bound was determined by Voigt modeling of the QCM-D data. Data are presented as mean ± SD (n = 4). Selected proteoglycan preparations were treated with C'ase ABC (-CS) and/or HepIII (-HS) prior to immobilization on the sensor surface and compared with the undigested fraction (control). *Asterisk* indicates significant difference compared with same cell type control or as indicated. *F*, schematic representation of LDL binding to the HS chains and protein cores present in the macrophage-derived proteoglycans. Mass of LDL bound to proteoglycans elaborated by (*G*) M1 polarized THP-1 cells following treatment with 1 M NaCl and (*H*) M2-polarized primary and THP-1 cells. The mass of LDL bound was determined by Voigt modeling of the QCM-D data. Data are presented as mean ± SD (n = 4). Selected proteoglycan preparations were treated with C'ase ABC (-CS) and/or HepIII (-HS) prior to immobilization on the sensor surface and compared with the undigested fraction (control). *Asterisk* indicates significant difference compared with same cell type control or as indicated. (I) Representative ΔD *versus* Δ*f* plot (D*f* plots) for LDL binding to M2 THP-1 proteoglycan preparations. The *arrow* indicates the time course of the data points.

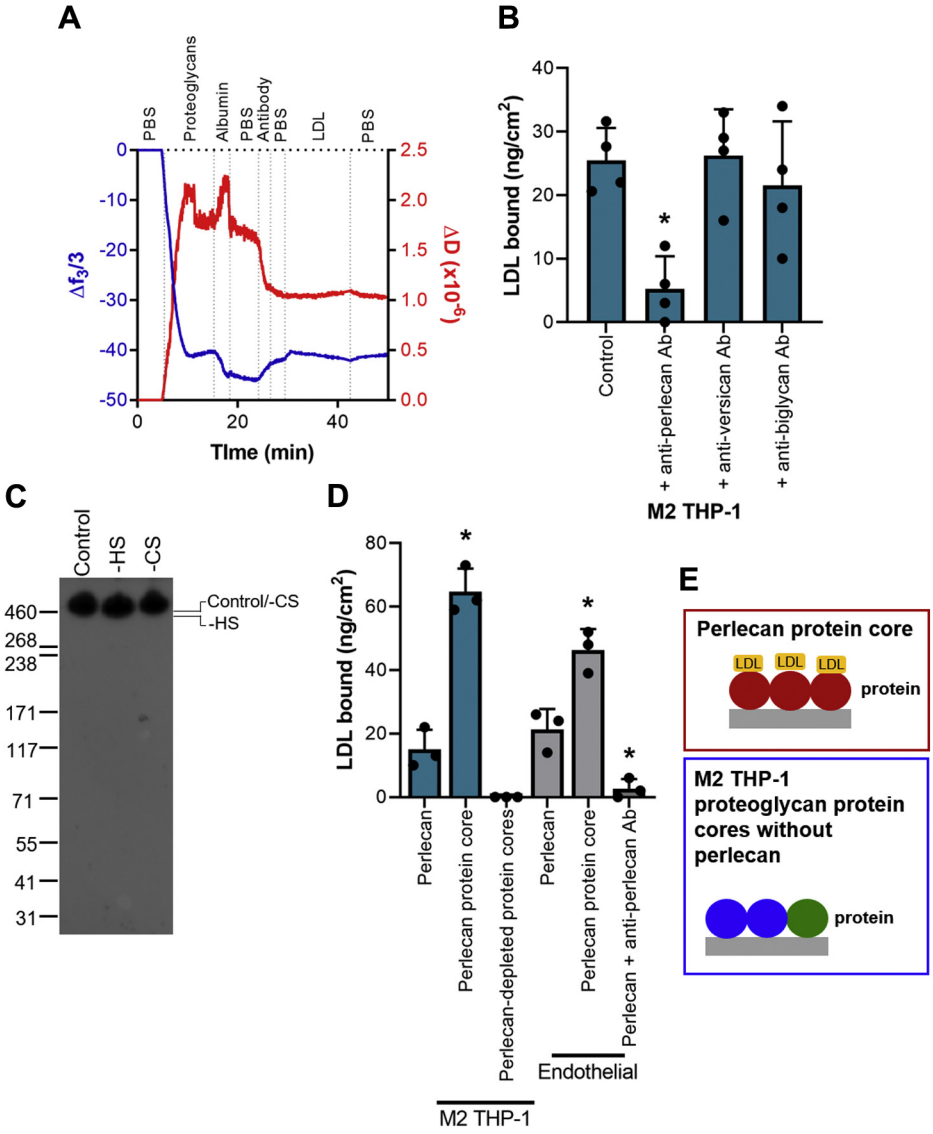

Figure 5. Perlecan binds LDL *via* the protein core. *A*, sample QCM-D experiment of LDL binding to M2 THP-1 proteoglycans displayed as changes in frequency (Δ*f*) and dissipation (ΔD) *versus* time for the third overtone. The vertical lines indicate the addition of PBS, proteoglycans, albumin, antibody, or LDL. *B*, mass of LDL bound to proteoglycans elaborated by M2-polarized THP-1 macrophages treated with both C'ase ABC (-CS) and HepIII (-HS) prior to immobilization followed by the addition of anti-perlecan, anti-versican, or anti-biglycan antibodies or no antibody (control). The mass of LDL bound was determined by Voigt modeling of the QCM-D data. Data are presented as mean ± SD (n = 4). *Asterisk* indicates significant difference compared with same cell type control. *C*, representative western blot of proteoglycan fraction elaborated by M2-polarized THP-1 macrophages either untreated (control) or treated with either HepIII (-HS) or C'ase ABC (-CS), electrophoresed on an 3–8% Tris-acetate gel, and probed for the presence of perlecan using a mouse monoclonal anti-perlecan antibody (clone E-6). Annotations on the right of the blot indicate the migration position of the lowest point of each band. *D*, mass of LDL bound to immunopurified perlecan derived from M2-polarized THP-1 cells compared with the M2 THP-1 fraction depleted of perlecan and glycosaminoglycans and immunopurified perlecan derived from human aortic endothelial cells. Selected experiments were performed after treatment of the proteoglycans with C'ase ABC and/or HepIII or addition of the anti-perlecan antibody. The mass of LDL bound was determined by Voigt modeling of the QCM-D data. Data are presented as mean ± SD (n = 4). *Asterisk* indicates significant difference compared with perlecan for the same cell type. *E*, schematic representation of LDL binding to the protein core of perlecan but not to the protein cores present in the proteoglycan fraction depleted of perlecan.

monosulfated disaccharides; however, it was not determined whether these contained 4- or 6-sulfated disaccharides. Importantly, 6-sulfated CS binds LDL, while 4-sulfated CS does not (58, 59), suggesting that the CS produced by macrophages may be mostly 4-sulfated. Moreover, the lack of LDL binding suggests that other cell types in the plaque are likely responsible for the deposition of CS proteoglycans that bind LDL.

This study found that the HS composition was sensitive to macrophage cell type and polarization. Proteoglycans produced by M1 macrophages had a higher level of HS chain sulfation compared with proteoglycans produced by M2 macrophages. In addition, HS produced by the THP-1 cells was more sulfated than for the primary cells. While there were subtle differences between the HS profile produced by primary and THP-1 cells, increased glycosaminoglycan chain sulfation has been reported in atherosclerosis and linked to increased LDL binding (60, 61). Furthermore, the spectrum of macrophage phenotypes within the plaque suggests that a range of HS structures will be present *in vivo* with a range of affinities for LDL.

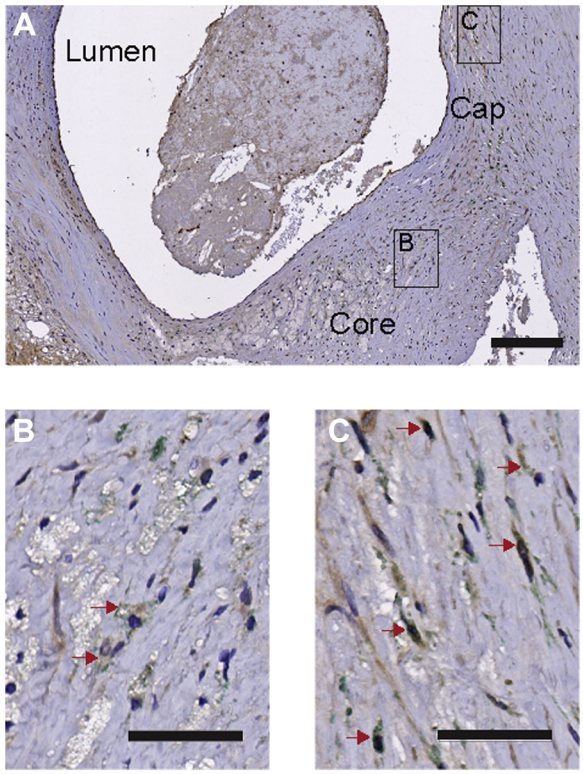

Figure 6. Perlecan colocalized with M2 macrophages in late atherosclerotic plaques. Representative micrographs showing the colocalization of perlecan and M2 macrophages at (*A*) low and (*B* and *C*) higher magnification of the boxed areas indicated in (*A*). Perlecan was probed with the rabbit polyclonal anti-perlecan antibody CCN-1 and visualized with DAB (brown). M2 macrophages were probed with the anti-CD163 antibody (clone 10D6) and visualized with Vina Green (*green*). Nuclei were counterstained with hematoxylin (*blue*). *Arrows* indicate regions of colocalization. Scale bar is 200 μm in (*A*) and 50 μm in (*B* and *C*).

The present study revealed that proteoglycans derived from M1 and M2 macrophages bound LDL *via* both the HS and protein core with M1 proteoglycans supporting a higher level of LDL binding than M2 proteoglycans. These data supported previous reports of more highly sulfated glycosaminoglycans binding LDL (13–16) as well as macrophage and smooth muscle cell–derived matrix binding LDL *via* HS (62, 63). However, the results presented here contrast with the reported LDL binding to M0 THP-1 macrophage-derived proteoglycans that was not HS-dependent (35).

Using antibodies to the protein core of selected proteoglycans that were abundant in the M2-derived proteoglycan fraction identified the protein core of perlecan as a major contributor to LDL binding. The perlecan core is reported to bind LDL *via* domain II, which is highly homologous to the lipid-binding region of the LDL receptor (32). While domain II of perlecan alone can bind LDL, the presence of regions outside of this domain, including domain I, increases LDL binding suggesting a cooperative effect of multiple regions within perlecan (32). Interestingly, more LDL bound to the protein core of perlecan in the absence of HS suggesting that the HS on perlecan did not support LDL binding and reduced access for LDL to the protein core. Similarly, LDL binding to the endothelial-derived matrix was enhanced after removal of the HS (64) and supports the findings presented here that LDL binding to perlecan was enhanced after removal of HS.

In this study, perlecan was localized to the fibrous cap and necrotic core in advanced human atherosclerotic plaques and aligned with previous studies of advanced atherosclerosis in murine models (31, 65) and nonhuman primates (56). In addition, perlecan colocalized with M2 macrophages and was localized to the same regions as HS extending previous findings (57). Notably, not all M2 macrophages colocalized with perlecan suggesting that other cell types also secreted this proteoglycan, most likely the resident smooth muscle and endothelial cells (49, 66).

The role of perlecan in atherosclerosis is likely context-dependent. Heterozygous deletion of perlecan leads to less atherosclerosis in young, but not old, apolipoprotein E-deficient (*ApoE0*) mice (31). This is thought to be due to the antiatherogenic properties of HS including through inhibition of LDL retention as observed in this study as well as modulation of smooth muscle cell proliferation (49, 57, 64). However, cross-breeding of the *ApoE0* mice with the HS-deficient perlecan ($Hspg2^{D3/D3}$) mice revealed a decrease in atherosclerotic lesions in both young and old mice, suggesting a proatherogenic role for HS (63). These contrasting findings suggest that the roles for HS go beyond lipid retention as the $ApoE0/Hspg2^{D3/D3}$ mice exhibited reduced smooth muscle cell populations in the lesions (63). In addition, the smooth muscle cell–derived matrix exhibited reduced LDL binding without HS (63), in contrast to the results presented in this study where both macrophage- and endothelial-derived perlecan supported higher LDL binding in the absence of HS. Together these suggest that the cell-type-dependent HS composition may contribute to the altered LDL-binding properties. Macrophages are involved in the progression of atherosclerosis through accelerating plaque formation (8–10), thus macrophage-derived proteoglycans, including HS and the protein core of perlecan, are likely involved in plaque progression rather than atherogenesis.

Atherosclerotic lesions contain both reduced HS and perlecan, but increased CS expression compared with normal vessels (30, 57). This is thought to be transcriptionally regulated as hypoxia increases perlecan expression by macrophage; but reduces its expression by endothelial cells (37, 67). In addition, hypoxia-inducible factor (HIF)-1a regulates perlecan gene expression while HIF-1a colocalizes with macrophages in atherosclerotic lesions (37, 68). In addition, HS biosynthesis is decreased in hypoxia, but not CS (51). Importantly, heparanase expression is increased in atherosclerosis (69) and may modulate HS retention and hence availability of LDL-binding sites. Together these studies suggest multiple regulation mechanisms for lipid retention by proteoglycans in atherosclerosis. While this study has focused on LDL binding, M2 macrophages are recognized for their stabilizing properties (40, 44, 46) as well as clearance of lipids (70, 71) suggesting that the association of M2 macrophages with perlecan and other proteoglycans in the lipid rich region of atherosclerotic plaques may be a mechanism of LDL clearance.

In summary, the present study is the first to establish a molecular basis for the interaction of LDL with proteoglycans secreted by polarized macrophages *in vitro*. Importantly, it implies that macrophages are likely to contribute to LDL retention in the plaque *via* protein and HS, but the way in which they do so is impacted by polarization as well as the presence of extracellular matrix degrading enzymes in the plaque. As such, the contribution of macrophages to LDL binding is complex. Due to the importance of glycosaminoglycans in mediating cellular processes in atherosclerosis, these findings should enable further studies aimed at elucidating the role of macrophage-derived proteoglycans in both pro-and antiatherogenic processes.

Experimental procedures

Reagents

Human buffy coat-derived monocytes were obtained under approval of the UNSW Human Research Ethics Committee from the Australian Red Cross Life Blood. The human monocytic cell line, THP-1, was also used as a source of monocytes when a larger number of cells were required. Chondroitinase ABC (C'ase ABC), heparinase III (HepIII), and mouse monoclonal antibody reactive to HS chains (clone 10E4) were purchased from Seikagaku Corp. The mouse monoclonal anti-perlecan antibody (clone E-6) was purchased from Santa Cruz Biotechnology while the mouse monoclonal anti-perlecan antibody (clone A74) was purchased from AbCam. A rabbit polyclonal anti-perlecan antibody (CCN-1) was raised in-house as previously described (49). Rabbit polyclonal antibodies against biglycan (catalogue no. LS-C341858) and versican (catalogue no. LS-C312902) were purchased from LSBio. Fluorophore-labeled monoclonal antibodies against CD86 (clone 2331) and CD11b (ICRF44) were purchased from BD Biosciences while a mouse monoclonal anti-CD163 antibody (clone 10D6) was purchased from Leica Microsystems. Biotinylated secondary anti-mouse and anti-rabbit antibodies were purchased from Merck-Millipore. Secondary horseradish-peroxidase-conjugated antibodies were purchased from Dako. IFN-γ was purchased from R&D systems. Human oxLDL was obtained from Alfa Aesar. Human LDL was purchased from STEMCELL Technologies Australia Pty Ltd, stored at 4 °C and used within 3 months. Dulbecco's phosphate buffered saline (PBS) did not contain divalent cations. All other chemicals were purchased from Sigma-Aldrich.

Immunohistochemistry

Sections (5 μm) of human atherosclerotic carotid tissues were obtained under ethics approval at Westmead Hospital, Australia. Sections were deparaffinized and rehydrated. Antigen retrieval was by heat using Borg decloaker solution in a decloaking chamber (Biocare Medical). Staining was carried out by an automated intelliPATH FLZ stainer in which the sections were firstly blocked with hydrogen peroxide followed by Background Sniper (all Biocare Medical). They were then incubated with primary antibodies, which were detected with the MACH 2 HRP-Polymer detection system (Biocare Medical). Counter staining was with hematoxylin. Tissue sections (n = 4 specimens) were stained with a mouse monoclonal anti-heparan sulfate antibody (clone 10E4, 2.0 μg/ml) and a mouse monoclonal anti-chondroitin sulfate antibody (clone CS-56, 2.0 μg/ml). Tissue sections (n = 3 specimens) were stained with both a rabbit polyclonal anti-perlecan antibody (CCN-1, 1:500 dilution) and a mouse monoclonal anti-CD163 antibody (0.5 μg/ml). Negative controls were performed simultaneously by incubating the sections with isotype control antibodies at the same concentration as the primary antibodies.

Culture and polarization of macrophages

THP-1 cells were maintained in standard medium containing RPM1-1640 medium supplemented with 10% fetal bovine serum and 1% (w/v) penicillin and streptomycin. Cells (3.3×10^5 cells/ml) were differentiated into naïve M0 macrophages by treatment with 5 ng/ml of phorbol-12-myristate 13-acetate (PMA) for 72 h in standard medium and cultured for a further 24 h in the absence of PMA prior to polarization. The macrophages were then polarized by incubation for 48 h with 100 ng/ml LPS and 20 ng/ml IFN-γ to produce M1 macrophages or polarized with 20 ng/ml IL-4 to produce M2 macrophages. M1 and M2 macrophages were transformed into foam cells by incubation with 50 μg/ml of oxLDL in serum-free RPMI-1640 containing the respective polarizing cytokines for 24 h (72). Cells were stained with Oil Red O and imaged under light microscopy.

Flow cytometry

Macrophages were harvested from tissue culture plates *via* a cell scraper. Cells (10^5) were suspended in PBS containing 1% (w/v) bovine serum albumin (BSA) for 10 min at room temperature followed by a 15 min incubation at room temperature with fluorophore-labeled monoclonal antibodies against CD86 or CD11b (BD Biosciences). Data were acquired on a flow cytometer (BD) for 10^5 events (n=2–5) and analyzed with FCS Express Version 4 software (De Novo Software).

Proteoglycan enrichment and perlecan immunopurification

Anion exchange chromatography using a diethylaminoethyl resin was used to isolate proteoglycans from medium conditioned by M1 or M2-polarized primary or THP-1 cells as previously described (49). Conditioned medium was pooled from three to ten medium changes to obtain a sufficient quantity of proteoglycans for analysis. Perlecan was isolated from selected macrophage fractions or human coronary artery endothelial cells using a monoclonal anti-perlecan domain I antibody (clone A71) affinity column, as previously described (66). Protein concentration was determined by the Coomassie protein assay and glycosaminoglycan concentration determined by the 1,9-Dimethylmethylene Blue assay (49, 73).

Mass spectrometry

Proteoglycan-enriched fractions in 25 mM ammonium bicarbonate were reduced (10 mM DTT, 10 min, 95 °C), alkylated

(25 mM iodoacetamide, 20 min, room temperature), and digested (sequencing grade trypsin, 20 μg/ml, 16 h, 37 °C). Samples were subjected to peptide analysis by liquid chromatography–tandem mass spectrometry (LC-MS^2) as previously described (74). Samples were analyzed by LC-MS^2 using an LTQ mass spectrometer (Thermo Fisher Scientific). The data was analyzed using the peaklist-generating software Mascot Daemon/extract_msn (version 2.5.1; Matrix Sciences) and the Mascot search engine (version 2.6.2) together with the NCBI sequence database with the homo sapiens taxonomy (November 2016 with 97,105,869 total sequences/309,980 human sequences in the database) with the following parameters: no fixed modifications; variable modifications = carbamidomethyl (C), oxidation (M) and propionamide (C); peptide mass tolerance = 4 ppm, fragment mass tolerance = 0.4 Da, maximum missed cleavages = 1; threshold score = MOWSE score >70.

ELISA

Proteoglycan-enriched samples (20 μg/ml) were probed with primary antibodies against perlecan (clone A74, 2 μg/ml), CS (clone CS-56, 2 μg/ml), or HS (clone 10E4, 2 μg/ml) as previously described (49).

Fluorophore-assisted Carbohydrate Electrophoresis (FACE)

FACE was performed on proteoglycan-enriched samples isolated from medium conditioned by M1 or M2-polarized primary or THP-1 cells as previously described (75).

Turbidity assay

Proteoglycan-enriched samples from M1 or M2-polarized THP-1 cells (0–25 μg/ml) were combined with 5 μg LDL in a final volume of 100 μl containing 0.05 M $CaCl_2$, pH 6 for 16 h at 37 °C. Measurement of the formation of insoluble complexes was performed as previously described (9).

Quartz crystal microbalance with dissipation monitoring (QCM-D)

A continuous flow of 0.1 ml/min and temperature of 37 °C were applied throughout the experiments using a QCM-D (Analyzer, Q-Sense). After a baseline was established with 10 mM PBS (pH 7.4, filtered and degassed), the sensor surfaces were coated with 2 μg of macrophage proteoglycans, blocked with bovine serum albumin (BSA, 2 mg/ml), washed with PBS, and then exposed to 5 μg of LDL followed by an additional PBS rinse. The binding of LDL was monitored by changes in frequency (Δf) and dissipation (ΔD) at the fundamental frequency as well as the 3rd–11th overtones and applied to the Voigt viscoelastic model to determine bound mass. Nonspecific interactions were monitored by adding LDL without proteoglycans. Variations on this protocol included treatment of fractions with either C'ase ABC (0.05 U/ml in 0.1 M Tris acetate, pH 8) or HepIII (0.01 U/ml in PBS) for 16 h at 37 °C prior to immobilization, the addition of polyclonal antibodies against perlecan (CCN-1, 1:1000), biglycan (2.0 μg/ml), or versican (2.0 μg/ml) following the immobilization of the proteoglycan preparations to determine the involvement of core protein in binding LDL, or the addition of 1 M NaCl after the last PBS rinse to examine whether the LDL-proteoglycan interaction was electrostatic.

Western blotting

Proteoglycan-enriched samples (5 μg/ml per lane) undigested or digested with either or both HepIII (0.01 U/ml in PBS) or C'ase ABC (0.05 U/ml in 0.1 M Tris acetate, pH 8) for 16 h at 37 °C were analyzed by western blotting using the mouse monoclonal anti-perlecan antibody (clone E-6, 0.2 μg/ml) as previously described (49).

Statistical analyses

Statistically significant differences were determined by one-way analysis of variance (ANOVA) and the Tukey post-test using GraphPad Prism. Data are expressed as mean ± standard deviation unless stated otherwise. Statistical significance was accepted at $p < 0.05$ and indicated by * in the figures.

Data availability

Mass spectrometry data files used in this article are available at MassIVE (https://massive.ucsd.edu/ProteoSAFe/static/massive.jsp, project ID: MSV000086746). All other data are contained within the article and supporting information.

Supporting information—This article contains supporting information.

Acknowledgments—We are grateful for the technical support from the Bioanalytical Mass Spectrometry Facility and Molecular Surface Interaction Network Laboratory, UNSW Sydney, which is in part funded by the Research Infrastructure program at UNSW as well as Virginia James (Westmead Hospital) for assistance with immunohistochemistry. This study was supported in part by grants from UNSW, Westmead Medical Research Foundation.

Author contributions—C. Y. N., J. M. W., H. W., H. J. M., and M. S. L. designed the research. C. Y. N. and H. N. K. conducted the experiments. C. Y. N., J. M. W., H. W., H. N. K., H. J. M., and M. S. L. analyzed the data. C. Y. N., H. J. M., and M. S. L. wrote the article; and all the authors reviewed and approved the final version of the article.

Funding and additional information—C. Y. N. was supported by an Australian Government Research Training Program Scholarship.

Conflict of interest—The authors declare that they have no conflicts of interest with the contents of this article.

Abbreviations—The abbreviations used are: CS, chondroitin sulfate; CSPG4, chondroitin sulfate proteoglycan 4; HIF, hypoxia-inducible factor; HS, heparan sulfate; LC-MS^2, liquid chromatography–tandem mass spectrometry; LDL, low-density lipoprotein; LPS, lipopolysaccharide; PBS, phosphate buffered saline; PMA, phorbol-12-myristate 13-acetate.

References

1. Hurt-Camejo, E., Olsson, U., Wiklund, O., Bondjers, G., and Camejo, G. (1997) Cellular consequences of the association of apoB lipoproteins with proteoglycans. Potential contribution to atherogenesis. *Arterioscler. Thromb. Vasc. Biol.* **17**, 1011–1017
2. Camejo, G., Lalaguna, F., Lopez, F., and Starosta, R. (1980) Characterization and properties of a lipoprotein-complexing proteoglycan from human aorta. *Atherosclerosis* **35**, 307–320
3. Kang, H., Lu, J., Yang, J., Fan, Y., and Deng, X. (2019) Interaction of arterial proteoglycans with low density lipoproteins (LDLs): From theory to promising therapeutic approaches. *Med. Novel Technology Devices* **3**, 100016
4. Ballinger, M. L., Ivey, M. E., Osman, N., Thomas, W. G., and Little, P. J. (2009) Endothelin-1 activates ETA receptors on human vascular smooth muscle cells to yield proteoglycans with increased binding to LDL. *Atherosclerosis* **205**, 451–457
5. Camejo, G., Fager, G., Rosengren, B., Hurt-Camejo, E., and Bondjers, G. (1993) Binding of low density lipoproteins by proteoglycans synthesized by proliferating and quiescent human arterial smooth muscle cells. *J. Biol. Chem.* **268**, 14131–14137
6. Hurt-Camejo, E., Camejo, G., Rosengren, B., López, F., Ahlström, C., Fager, G., and Bondjers, G. (1992) Effect of arterial proteoglycans and glycosaminoglycans on low density lipoprotein oxidation and its uptake by human macrophages and arterial smooth muscle cells. *Arterioscler. Thromb.* **12**, 569–583
7. Borén, J., and Williams, K. J. (2016) The central role of arterial retention of cholesterol-rich apolipoprotein-B-containing lipoproteins in the pathogenesis of atherosclerosis: A triumph of simplicity. *Curr. Opin. Lipidol.* **27**, 473–483
8. Navab, M., Berliner, J. A., Watson, A. D., Hama, S. Y., Territo, M. C., Lusis, A. J., Shih, D. M., Van Lenten, B. J., Frank, J. S., Demer, L. L., Edwards, P. A., and Fogelman, A. M. (1996) The yin and yang of oxidation in the development of the fatty streak. *Arterioscler. Thromb. Vasc. Biol.* **16**, 831–842
9. Hurt, E., Bondjers, G., and Camejo, G. (1990) Interaction of LDL with human arterial proteoglycans stimulates its uptake by human monocyte-derived macrophages. *J. Lipid Res.* **31**, 443–454
10. Osterud, B., and Bjorklid, E. (2003) Role of monocytes in atherogenesis. *Physiol. Rev.* **83**, 1069–1112
11. Cushing, S. D., Berliner, J. A., Valente, A. J., Territo, M. C., Navab, M., Parhami, F., Gerrity, R., Schwartz, C. J., and Fogelman, A. M. (1990) Minimally modified low density lipoprotein induces monocyte chemotactic protein 1 in human endothelial cells and smooth muscle cells. *Proc. Natl. Acad. Sci. U. S. A.* **87**, 5134–5138
12. Iozzo, R. V., and Schaefer, L. (2015) Proteoglycan form and function: A comprehensive nomenclature of proteoglycans. *Matrix Biol.* **42**, 11–55
13. Mahley, R. W., Weisgraber, K. H., and Innerarity, T. L. (1979) Interaction of plasma lipoproteins containing apolipoproteins B and E with heparin and cell surface receptors. *Biochim. Biophys. Acta* **575**, 81–91
14. Camejo, G., Olofsson, S., Lopez, F., Carlsson, P., and Bondjers, G. (1988) Identification of Apo B-100 segments mediating the interaction of low density lipoproteins with arterial proteoglycans. *Atherosclerosis* **8**, 368–377
15. Iverius, P. H. (1972) The interaction between human plasma lipoproteins and connective tissue glycosaminoglycans. *J. Biol. Chem.* **247**, 2607–2613
16. Borén, J., Olin, K., Lee, I., Chait, A., Wight, T. N., and Innerarity, T. L. (1998) Identification of the principal proteoglycan-binding site in LDL: A single-point mutation in apo-B100 severely affects proteoglycan interaction without affecting LDL receptor binding. *J. Clin. Invest.* **101**, 2658–2664
17. Krisko, A., Piantanida, I., Kveder, M., Pifat, G., Lee, A., Greilberger, J., Kipmen-Korgun, D., and Jurgens, G. (2006) The effect of heparin on structural and functional properties of low density lipoproteins. *Biophys. Chem.* **119**, 234–239
18. Pan, Y. T., Kruski, A. W., and Elbein, A. D. (1978) Binding of [3H]heparin to human plasma low density lipoprotein. *Arch. Biochem. Biophys.* **189**, 231–240
19. Owens, R. T., and Wagner, W. D. (1991) Proteoglycans produced by cholesterol-enriched macrophages bind plasma low density lipoprotein. *Atherosclerosis* **91**, 229–240
20. Brown, M. S., Basu, S. K., Falck, J. R., Ho, Y. K., and Goldstein, J. L. (1980) The scavenger cell pathway for lipoprotein degradation: Specificity of the binding site that mediates the uptake of negatively-charged LDL by macrophages. *J. Supramol. Struct.* **13**, 67–81
21. Kaplan, M., and Aviram, M. (2000) Macrophage plasma membrane chondroitin sulfate proteoglycan binds oxidized low-density lipoprotein. *Atherosclerosis* **149**, 5–17
22. Halvorsen, B., Aas, U. K., Kulseth, M. A., Drevon, C. A., Christiansen, E. N., and Kolset, S. O. (1998) Proteoglycans in macrophages: Characterization and possible role in the cellular uptake of lipoproteins. *Biochem. J.* **331**(Pt 3), 743–752
23. Osman, N., Grande-Allen, K. J., Ballinger, M. L., Getachew, R., Marasco, S., O'Brien, K. D., and Little, P. J. (2013) Smad2-dependent glycosaminoglycan elongation in aortic valve interstitial cells enhances binding of LDL to proteoglycans. *Cardiovasc. Pathol.* **22**, 146–155
24. Christner, J. E. (1988) Biosynthesis of chondroitin sulfate proteoglycan by P388D1 macrophage-like cell line. *Arteriosclerosis* **8**, 535–543
25. Chang, M. Y., Olin, K. L., Tsoi, C., Wight, T. N., and Chait, A. (1998) Human monocyte-derived macrophages secrete two forms of proteoglycan-macrophage colony-stimulating factor that differ in their ability to bind low density lipoproteins. *J. Biol. Chem.* **273**, 15985–15992
26. Dalferes, E. R., Jr., Radhakrishnamurthy, B., Ruiz, H. A., and Berenson, G. S. (1987) Composition of proteoglycans from human atherosclerotic lesions. *Exp. Mol. Pathol.* **47**, 363–376
27. Kovanen, P. T., and Pentikainen, M. O. (1999) Decorin links low-density lipoproteins (LDL) to collagen: A novel mechanism for retention of LDL in the atherosclerotic plaque. *Trends Cardiovasc. Med.* **9**, 86–91
28. Adhikara, I. M., Yagi, K., Mayasari, D. S., Ikeda, K., Kitagawa, H., Miyata, O., Igarashi, M., Hatakeyama, K., Asada, Y., Hirata, K.-i., and Emoto, N. (2019) Chondroitin sulfate N-acetylgalactosaminyltransferase-2 deletion alleviates lipoprotein retention in early atherosclerosis and attenuates aortic smooth muscle cell migration. *Biochem. Biophys. Res. Commun.* **509**, 89–95
29. Volker, W., Schmidt, A., Oortmann, W., Broszey, T., Faber, V., and Buddecke, E. (1990) Mapping proteoglycans in atherosclerotic lesions. *Eur. Heart J* **11 Suppl E**, 29–40
30. Hollmann, J., Schmidt, A., von Bassewitz, D. B., and Buddecke, E. (1989) Relationship of sulfated glycosaminoglycans and cholesterol content in normal and arteriosclerotic human aorta. *Arteriosclerosis* **9**, 154–158
31. Vikranadithyan, R. K., Kako, Y., Chen, G., Hu, Y., Arikawa-Hirasawa, E., Yamada, Y., and Goldberg, I. J. (2004) Atherosclerosis in perlecan heterozygous mice. *J. Lipid Res.* **45**, 1806–1812
32. Xu, Y. X., Ashline, D., Tassa, C., Shaw, S. Y., Ravid, K., Layne, M. D., Reinbold, V., and Robbins, P. W. (2015) The glycosylation-dependent interaction of perlecan core protein with LDL: Implications for atherosclerosis. *J. Lipid Res.* **56**, 266–276
33. Little, P. J., Tannock, L., Olin, K. L., Chait, A., and Wight, T. N. (2002) Proteoglycans synthesized by arterial smooth muscle cells in the presence of transforming growth factor-b1 exhibit increased binding to LDLs. *Arterioscler. Thromb. Vasc. Biol.* **22**, 55–60
34. Vijayagopal, P., and Menon, P. V. (2005) Varied low density lipoprotein binding property of proteoglycans synthesized by vascular smooth muscle cells cultured on extracellular matrix. *Atherosclerosis* **178**, 75–82
35. Olsson, U., Ostergren-Lunden, G., and Moses, J. (2001) Glycosaminoglycan-lipoprotein interaction. *Glycoconj. J.* **18**, 789–797
36. Asplund, A., Friden, V., Stillemark-Billton, Camejo, G., and Bondjers, G. (2011) Macrophages exposed to hypoxia secrete proteoglycans for which LDL has higher affinity. *Atherosclerosis* **215**, 77–81
37. Asplund, A., Stillemark-Billton, Larsson, E., Rydberg, E. K., Moses, J., Hulten, L. M., Fagerberg, B., Camejo, G., and Bondjers, G. (2010) Hypoxia regulation of secreted proteoglycans in macrophages. *Glycobiology* **20**, 33–40
38. Hamilton, T. A., Ohmori, Y., Tebo, J. M., and Kishore, R. (1999) Regulation of macrophage gene expression by pro- and anti-inflammatory cytokines. *Pathobiology* **67**, 241–244
39. Martinez, F. O., Sica, A., Mantovani, A., and Locati, M. (2008) Macrophage activation and polarization. *Front. Biosci.* **13**, 453–461
40. Gordon, S. (2003) Alternative activation of macrophages. *Nat. Rev. Immunol.* **3**, 23–35

41. Mills, C. D., Kincaid, K., Alt, J. M., Heilman, M. J., and Hill, A. M. (2000) M-1/M-2 macrophages and the Th1/Th2 paradigm. *J. Immunol.* **164**, 6166–6173
42. Stoger, J. L., Gijbels, M. J., van der Velden, S., Manca, M., van der Loos, C. M., Biessen, E. A., Daemen, M. J., Lutgens, E., and de Winther, M. P. (2012) Distribution of macrophage polarization markers in human atherosclerosis. *Atherosclerosis* **225**, 461–468
43. Chinetti-Gbaguidi, G., Colin, S., and Staels, B. (2015) Macrophage subsets in atherosclerosis. *Nat. Rev. Cardiol.* **12**, 10–17
44. Medbury, H. J., James, V., Ngo, J., Hitos, K., Wang, Y., Harris, D. C., and Fletcher, J. P. (2013) Differing association of macrophage subsets with atherosclerotic plaque stability. *Int. Angiol* **32**, 74–84
45. Bi, Y., Chen, J., Hu, F., Liu, J., Li, M., and Zhao, L. (2019) M2 macrophages as a potential target for antiatherosclerosis treatment. *Neural Plasticity* **2019**, 6724903
46. Zhang, X., Liu, M. H., Qiao, L., Zhang, X. Y., Liu, X. L., Dong, M., Dai, H. Y., Ni, M., Luan, X. R., Guan, J., and Lu, H. X. (2018) Ginsenoside Rb1 enhances atherosclerotic plaque stability by skewing macrophages to the M2 phenotype. *J. Cell Mol. Med.* **22**, 409–416
47. Qin, Z. (2012) The use of THP-1 cells as a model for mimicking the function and regulation of monocytes and macrophages in the vasculature. *Atherosclerosis* **221**, 2–11
48. Tedesco, S., De Majo, F., Kim, J., Trenti, A., Trevisi, L., Fadini, G. P., Bolego, C., Zandstra, P. W., Cignarella, A., and Vitiello, L. (2018) Convenience versus biological significance: Are PMA-differentiated THP-1 cells a reliable substitute for blood-derived macrophages when studying *in vitro* polarization? *Front. Pharmacol.* **9**, 71
49. Lord, M. S., Chuang, C. Y., Melrose, J., Davies, M. J., Iozzo, R. V., and Whitelock, J. M. (2014) The role of vascular-derived perlecan in modulating cell adhesion, proliferation and growth factor signaling. *Matrix Biol.* **35**, 112–122
50. Rey-Giraud, F., Hafner, M., and Ries, C. H. (2012) *In vitro* generation of monocyte-derived macrophages under serum-free conditions improves their tumor promoting functions. *PLoS One* **7**, e42656
51. Asplund, A., Ostergren-Lunden, G., Camejo, G., Stillemark-Billton, and Bondjers, G. (2009) Hypoxia increases macrophage motility possibly by decreasing the heparan sulfate proteoglycan biosynthesis. *J. Leukoc. Biol.* **86**, 381–388
52. Swart, M., and Troeberg, L. (2019) Effect of polarization and chronic inflammation on macrophage expression of heparan sulfate proteoglycans and biosynthesis enzymes. *J. Histochem. Cytochem.* **67**, 9–27
53. Chang, M. Y., Tanino, Y., Vidova, V., Kinsella, M. G., Chan, C. K., Johnson, P. Y., Wight, T. N., and Frevert, C. W. (2014) A rapid increase in macrophage-derived versican and hyaluronan in infectious lung disease. *Matrix Biol.* **34**, 1–12
54. Mikita, T., Porter, G., Lawn, R. M., and Shiffman, D. (2001) Oxidized low density lipoprotein exposure alters the transcriptional response of macrophages to inflammatory stimulus. *J. Biol. Chem.* **276**, 45729–45739
55. Hakamata, H., Miyazaki, A., Sakai, M., Sakamoto, Y. I., and Horiuchi, S. (1998) Cytotoxic effect of oxidized low density lipoprotein on macrophages. *J. Atheroscler. Thromb.* **5**, 66–75
56. Evanko, S. P., Raines, E. W., Ross, R., Gold, L. I., and Wight, T. N. (1998) Proteoglycan distribution in lesions of atherosclerosis depends on lesion severity, structural characteristics, and the proximity of platelet-derived growth factor and transforming growth factor-b. *Am. J. Pathol.* **152**, 533–546
57. Tran, P. K., Agardh, H. E., Tran-Lundmark, K., Ekstrand, J., Roy, J., Henderson, B., Gabrielsen, A., Hansson, G. K., Swedenborg, J., Paulsson-Berne, G., and Hedin, U. (2007) Reduced perlecan expression and accumulation in human carotid atherosclerotic lesions. *Atherosclerosis* **190**, 264–270
58. Little, P. J., Osman, N., and O'Brien, K. D. (2008) Hyperelongated biglycan: The surreptitious initiator of atherosclerosis. *Curr. Opin. Lipidol.* **19**, 448–454
59. Srinivasan, S. R., Xu, J. H., Vijayagopal, P., Radhakrishnamurthy, B., and Berenson, G. S. (1995) Low-density lipoprotein binding affinity of arterial chondroitin sulfate proteoglycan variants modulates cholesteryl ester accumulation in macrophages. *Biochim. Biophys. Acta* **1272**, 61–67
60. Stevens, R. L., Colombo, M., Gonzales, J. J., Hollander, W., and Schmid, K. (1976) The glycosaminoglycans of the human artery and their changes in atherosclerosis. *J. Clin. Invest.* **58**, 470–481
61. Wasty, F., Alavi, M. Z., and Moore, S. (1993) Distribution of glycosaminoglycans in the intima of human aortas: Changes in atherosclerosis and diabetes mellitus. *Diabetologia* **36**, 316–322
62. Kaplan, M., and Aviram, M. (1997) Oxidized LDL binding to a macrophage-secreted extracellular matrix. *Biochem. Biophys. Res. Commun.* **237**, 271–276
63. Tran-Lundmark, K., Tran, P.-K., Paulsson-Berne, G., Fridén, V., Soininen, R., Tryggvason, K., Wight, T. N., Kinsella, M. G., Borén, J., and Hedin, U. (2008) Heparan sulfate in perlecan promotes mouse atherosclerosis: Roles in lipid permeability, lipid retention, and smooth muscle cell proliferation. *Circ. Res.* **103**, 43–52
64. Pillarisetti, S., Paka, L., Obunike, J. C., Berglund, L., and Goldberg, I. J. (1997) Subendothelial retention of lipoprotein (a). Evidence that reduced heparan sulfate promotes lipoprotein binding to subendothelial matrix. *J. Clin. Invest.* **100**, 867–874
65. Kunjathoor, V. V., Chiu, D. S., O'Brien, K. D., and LeBoeuf, R. C. (2002) Accumulation of biglycan and perlecan, but not versican, in lesions of murine models of atherosclerosis. *Arterioscler. Thromb. Vasc. Biol.* **22**, 462–468
66. Whitelock, J. M., Graham, L. D., Melrose, J., Murdoch, A. D., Iozzo, R. V., and Anne Underwood, P. (1999) Human perlecan immunopurified from different endothelial cell sources has different adhesive properties for vascular cells. *Matrix Biol.* **18**, 163–178
67. Li, Y. Z., Liu, X. H., and Cai, L. R. (2007) Down-regulation of perlecan expression contributes to the inhibition of rat cardiac microvascular endothelial cell proliferation induced by hypoxia. *Sheng Li Xue Bao* **59**, 221–226
68. Sluimer, J. C., Gasc, J. M., van Wanroij, J. L., Kisters, N., Groeneweg, M., Sollewijn Gelpke, M. D., Cleutjens, J. P., van den Akker, L. H., Corvol, P., Wouters, B. G., Daemen, M. J., and Bijnens, A. P. (2008) Hypoxia, hypoxia-inducible transcription factor, and macrophages in human atherosclerotic plaques are correlated with intraplaque angiogenesis. *J. Am. Coll. Cardiol.* **51**, 1258–1265
69. Baker, A. B., Chatzizisis, Y. S., Beigel, R., Jonas, M., Stone, B. V., Coskun, A. U., Maynard, C., Rogers, C., Koskinas, K. C., Feldman, C. L., Stone, P. H., and Edelman, E. R. (2010) Regulation of heparanase expression in coronary artery disease in diabetic, hyperlipidemic swine. *Atherosclerosis* **213**, 436–442
70. Cardilo-Reis, L., Gruber, S., Schreier, S. M., Drechsler, M., Papac-Milicevic, N., Weber, C., Wagner, O., Stangl, H., Soehnlein, O., and Binder, C. J. (2012) Interleukin-13 protects from atherosclerosis and modulates plaque composition by skewing the macrophage phenotype. *EMBO Mol. Med.* **4**, 1072–1086
71. Barthwal, M. K., Anzinger, J. J., Xu, Q., Bohnacker, T., Wymann, M. P., and Kruth, H. S. (2013) Fluid-phase pinocytosis of native low density lipoprotein promotes murine M-CSF differentiated macrophage foam cell formation. *PLoS One* **8**, e58054
72. van Tits, L. J., Stienstra, R., van Lent, P. L., Netea, M. G., Joosten, L. A., and Stalenhoef, A. F. (2011) Oxidized LDL enhances pro-inflammatory responses of alternatively activated M2 macrophages: A crucial role for Krüppel-like factor 2. *Atherosclerosis* **214**, 345–349
73. Davies, N. P., Roubin, R. H., and Whitelock, J. M. (2008) Characterization and purification of glycosaminoglycans from crude biological samples. *J. Agric. Food Chem.* **56**, 343–348
74. Lord, M. S., Day, A. J., Youssef, P., Zhuo, L., Watanabe, H., Caterson, B., and Whitelock, J. M. (2013) Sulfation of the bikunin chondroitin sulfate chain determines heavy chain.hyaluronan complex formation. *J. Biol. Chem.* **288**, 22930–22941
75. Lord, M. S., Cheng, B., Tang, F., Lyons, J. G., Rnjak-Kovacina, J., and Whitelock, J. M. (2016) Bioengineered human heparin with anticoagulant activity. *Metab. Eng.* **38**, 105–114